Integration of Multimodal Neuroimaging and Electroencephalography for the Study of Acute Epileptiform Activity After Traumatic Brain Injury

Andrei Irimia[1], Sheng-Yang M. Goh[1], Paul M. Vespa[2], and John D. Van Horn[1(✉)]

[1] Laboratory of Neuro Imaging, Institute for Neuroimaging and Informatics, University of Southern California, Los Angeles, CA, USA
{andrei.irimia,matthew.goh,jack.vanhorn}@loni.usc.edu
[2] Brain Injury Research Center and Departments of Neurology and Neurosurgery, University of California, Los Angeles, CA, USA
pvespa@mednet.ucla.edu

Abstract. The integration of multidimensional, longitudinal data acquired using the combined use of structural neuroimaging [e.g. magnetic resonance imaging (MRI), computed tomography (CT)] and neurophysiological recordings [e.g. electroencephalography (EEG)] poses substantial challenges to neuroinformaticians and to biomedical scientists who interact frequently with such data. In traumatic brain injury (TBI) studies, this challenge is even more severe due to the substantial heterogeneity of TBIs across patients and to the variety of neurophysiological responses to injury. Additionally, the study of acute epileptiform activity prompted by TBI poses logistic, analytic and data integration difficulties. Here we describe our proposed solutions to the integration of structural neuroimaging with neurophysiological recordings to study epileptiform activity after TBI. Based on techniques for TBI-robust segmentation and electrical activity localization, we have developed an approach to the joint analysis of MRI/CT/EEG data to identify the foci of seizure-related activity and to facilitate the study of TBI-related neuropathophysiology.

Keywords: Magnetic resonance imaging · Computed tomography · Electroencephalography · Traumatic brain injury · Big data · Segmentation · Seizure · Neurophysiology

1 Introduction

The advent and proliferation of multimodal neuroimaging approaches for the study of brain structure and function have greatly facilitated both clinical and basic science advances. With such progress, however, has also come the necessity to accommodate, share, process and analyze very large amounts of data. Neuroimaging scans acquired using techniques such as magnetic resonance imaging (MRI) and computed tomography (CT) have the advantage of relatively high spatial resolution, though simultaneously the potential disadvantage of requiring large amounts of data storage and of computationally-intensive algorithms for their analysis. Techniques such as functional MRI (fMRI)

N. Ashish and J.-L. Ambite (Eds.): DILS 2015, LNBI 9162, pp. 165–179, 2015.
DOI: 10.1007/978-3-319-21843-4_13

involve the acquisition of four-dimensional (4D) data (3 spatial dimensions and time), leading to even higher demands from the standpoint of data storage and computation. On the other hand, neurophysiological recordings acquired using methods such as electroencephalography (EEG) benefit from high temporal resolution (on the order of milliseconds), though they suffer from relatively poor spatial resolution compared to MRI. Nevertheless, the use of anatomically-informed inverse localization procedures [1] has greatly widened the horizon of applicability for EEG, though at the expense of compounded, multiplicative increases in data storage allocation and computational time requirements. For these reasons, improved approaches to the problems of storage, management, sharing and analysis of combined MRI/CT/EEG recordings are necessary.

The task of multimodal neuroimaging data integration and joint analysis is particularly challenging in studies of traumatic brain injury (TBI), where the structural profile of the brain can change dramatically over the days and even hours following injury. In TBI patients, large alterations in the biochemical, neurophysiologic and metabolic activity of the brain can occur very rapidly and may require immediate clinical intervention and monitoring. For this reason, neuroimaging the TBI brain to inform clinical decision-making can necessitate frequent acquisition of CT and MRI scans to monitor injury evolution and to formulate appropriate treatments. What is more, TBI is a very heterogeneous condition because the spatiotemporal profiles of brain lesions are extremely difficult to quantify without substantial input from neuroimaging technologies.

Electrophysiological recordings via continuous EEG (cEEG) are used routinely in neurointensive care units to identify changes in the baseline electrical activity of the brain as well as neuropathophysiological manifestations such as epileptiform spiking, seizures, and more serious conditions such *status epilepticus* [2]. Other monitoring techniques which are used routinely in neurointensive care units include magnetic resonance spectroscopy (MRS), blood assays, depth electrode recordings, positron emission tomography (PET), etc. The integration, analysis, and interpretation of data being made available from so many sources can pose substantial challenges not only to clinicians but also to biomedical researchers who aim to integrate, analyze and translate basic findings about TBI into information which has broad bedside relevance and applicability.

In this paper, we aim to describe our proposed solutions to the task of integrating structural neuroimaging with neurophysiological recordings to study epileptiform activity prompted by TBI. Based on techniques which we and our collaborators have pioneered for the purpose of TBI-robust segmentation and electrical activity localization, we have developed a set of approaches for the joint analysis of MRI/CT/EEG data acquired from TBI patients. The integration of these methods across modalities can facilitate the study of TBI-related neuropathophysiology by identifying and analyzing the spatiotemporal properties of seizure-related activity and can contribute to the formulation of TBI patient-tailored interventions and treatments.

2 Methodologies

In what follows, a series of integrated techniques for the acquisition, analysis and interpretation of MRI/CT/EEG data acquired from TBI patients are illustrated.

The approaches described below have resulted from over half a decade of collaborative research between the Laboratory of Neuro Imaging (LONI) and Institute for Neuroimaging and Informatics (INI) at the University of Southern California and the Brain Injury Research Center (BIRC) at the University of California, Los Angeles. In addition to detailed descriptions of the analysis steps involved, we outline some of our numerous challenges and potential solutions for the integration of vastly different neuroimaging modalities in the attempt to combine knowledge of brain structure with information provided by neurophysiology techniques.

2.1 Neuroimaging Data Acquisition

Before studies are conducted, each patient or her/his legally-authorized representative provides informed written consent as required by the Declaration of Helsinki, U.S. 45 CFR 46. Neuroimage volume acquisition is conducted with the approval of the local ethics committees at the research institution where data are acquired. Brain imaging data sets are fully anonymized and stored on the LONI Image Data Archive (IDA), and no linked coding or keys to subject identity are maintained.

One important feature of the approach we use for neuroimaging data integration is that it accommodates multimodally-acquired data. This is very helpful in studies of TBI, where more than one MRI acquisition sequences are often required to identify the nature and extent of pathology. In our own studies, MRI volumes are acquired at 3.0 T using a Trio TIM scanner (Siemens Corp., Erlangen, Germany), although various field strengths, voxel sizes and sequence parameters can be used. The acquisition protocol is designed to optimize the amount of information which can be inferred from multimodal MRI, while minimizing the amount of time which the patient must spend in the scanner. The protocol itself consists of magnetization prepared rapid acquisition gradient echo (MP-RAGE) T_1-weighted imaging, fluid attenuated inversion recovery (FLAIR), turbo spin echo (TSE) T_2-weighted imaging, gradient recalled echo (GRE) T_2-weighted imaging and susceptibility-weighted imaging (SWI; see Fig. 1). For T_1-weighted volumes, typical acquisition parameters include a repetition time (TR) of 1900 ms, an echo time (TE) of 3.52 ms, a flip angle (FA) of 9 degrees, an inversion time (TI) of 900 ms, a voxel size of 1 mm^3, a phase field of view (FOV) of 100 %, a matrix size of $256 \times 256 \times 256$ and 100 % sampling. A detailed list of typical parameters for the other sequence types is provided in [2]. For diffusion tensor imaging (DTI), volumes with up to 68 diffusion gradient directions are typically acquired using a 12-channel coil and a sequence with the following parameters: TR = 9.4 s, TE = 88 ms, flip angle = 90°, voxel size = 2 mm^3, acquisition matrix = $128 \times 128 \times 128$. Two non-diffusion weighted volumes are usually acquired for each patient (B_0 values: 0 s/mm^2 and 1,000 s/mm^2). Conventional computed tomography (CT) scans are also obtained. Continuous electroencephalographic (cEEG) measurements are acquired and monitored continuously at the patient's bedside starting immediately after admission to the neurointensive care unit (NICU).

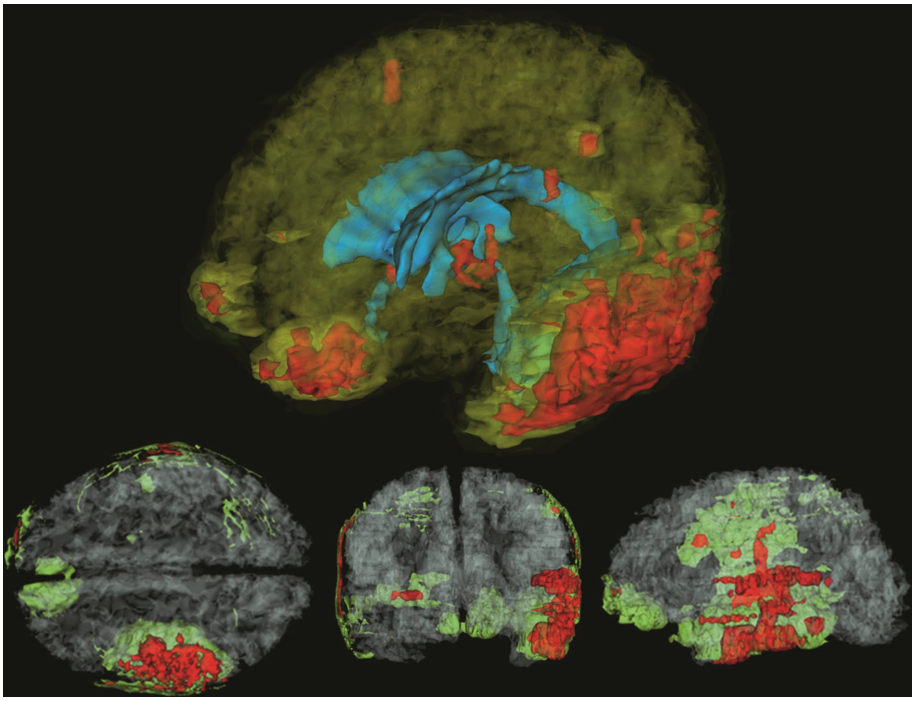

Fig. 1. Visualization of a TBI brain, showing healthy-appearing GM/WM (translucent), the ventricular system (blue), edema (green), and hemorrhage (red) (Color figure onlilne).

2.2 MRI Processing

Prior to any analysis, MRI, CT and DTI volumes are co-registered using a 12-parameter affine registration. Image processing is performed using the LONI Pipeline environment (pipeline.loni.usc.edu), including operations such as bias field correction, skull stripping, and multimodal volume co-registration. Hemorrhagic tissues are segmented from SWI and GRE T_2-weighted volumes, whereas edematous tissues are segmented from TSE T_2–weighted and FLAIR volumes (see Fig. 1). The details of the procedure for pathology identification are detailed elsewhere [4]. FreeSurfer (freesurfer.net) is utilized to segment healthy-appearing white matter (WM), grey matter (GM), and cerebrospinal fluid (CSF) from T_1–weighted volumes, as well as to perform regional parcellation [5, 6]. Briefly, the cortical surface of each patient is reconstructed as a triangular tessellation with an average inter-vertex distance of ~1 mm to produce a high-resolution, smooth representation of the WM/GM interface [7]. At each tessellation vertex, cortical thickness is measured as the distance between the cortical surface and the WM/GM boundary. A total of 74 cortical structures (gyri and sulci) are identified and parceled using a probabilistic atlas [8]. Neuroanatomical labels are assigned to voxels based on probabilistic information

estimated from a manually-labeled training set; this method uses the previous probability of a tissue class occurring at a specific atlas location as well as the probability of the local spatial configuration of labels given each tissue class. The technique is comparable in accuracy with manual labeling [9].

TBI-related lesions are segmented from GRE/SWI/FLAIR volumes as outlined elsewhere [10, 11], the scalp is segmented from T_1–weighted MRI, and hard bone is segmented from CT volumes. Eyes, muscle, cartilage, mucus, nerves, teeth, and ventriculostomy shunts are labeled based on T_1/T_2 MRI. 3D models for all tissue type are generated in 3D Slicer (slicer.org), which is also used to generate 3D models and visualizations of TBI-related pathology and of healthy-appearing tissues. Manual correction of segmentation errors is performed by three experienced users with training in neuroanatomy.

2.3 DTI Processing

For DTI, eddy current correction is first applied to each volume, which is subsequently processed using TrackVis (trackvis.org) as well with the Diffusion ToolKit to reconstruct fiber tracts using deterministic tractography. A brain mask is first created using FSL [12] to minimize extra-cerebral noise, and TrackVis is then used to reconstruct and to render fiber tracts, which can subsequently be loaded and viewed in 3D Slicer or using other tractography visualization software. Fiber bundles shorter than 1.5 cm are discarded. Fiber tracts which do not intersect pathology-affected regions can be discarded. To reconstruct tracts of specific interest, seed regions can placed in particular locations (such as the brain stem and the internal capsule in the case of the corticospinal tract, CST), and the WM tracts intersecting these regions can then be isolated (Fig. 2).

2.4 Longitudinal Structural Analysis

Importantly, longitudinal studies can be accommodated in our approach. For example, in a typical study, scanning sessions are held both several days (acute baseline) as well as 6 months (chronic follow-up) after TBI, and the same MRI scanner and acquisition parameters are used in both cases. Lesion volumes are measured in cubic centimeters based on pathology models created in 3D Slicer or ITKSnap (itksnap.org). The percentages of longitudinal volumetric changes in pathology as well as in healthy-appearing WM and GM are calculated as $(v_{i+1} - v_i)/v_i$, where v_i and v_{i+1} are the volumes of the respective structures at times i and $i + 1$, respectively (Fig. 4).

Several ways to analyze longitudinal changes in WM connections are available in our environment. To quantify the manner and extent to which fibers are affected by pathology, the sum over the lengths of fibers intersecting pathology-affected regions can be divided by the sum of the lengths of fibers in the whole brain, thereby yielding the percentage of WM connections in the brain which intersect the primary injury. This is useful because it provides useful information on how broadly DAI may have affected each patient. Alternatively, changes in connectivity strength between different regions can be investigated to determine how severely the wiring of the brain has been affected by TBI. Finally, changes in the ratio of T1 to T2-weighted image intensities can provide a surrogate measure of axonal demyelination [13], which allows us to study long-term effects of brain injuries (Fig. 3).

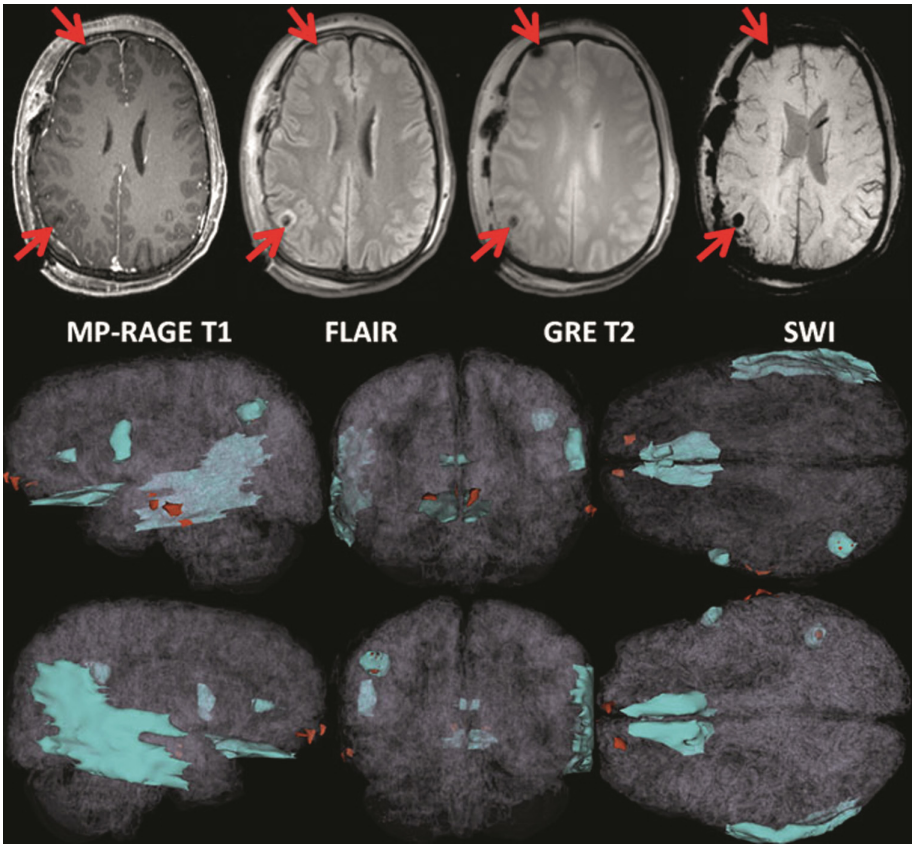

Fig. 2. (A) Sample MRI slices acquired from a typical TBI patient using various sequences. Arrows indicate the locations of primary injuries. (B) Translucent models of the WM and GM (as reconstructed based on the segmentation) with edema (cyan) and hemorrhage (red) shown using opaque 3D models. Note the fronto-temporal spatial distribution of the injuries, typical in TBI (Color figure onlilne).

2.5 EEG Forward Modeling

Integrating structural MRI, CT and DTI data with neurophysiological recordings poses daunting complexities in the context of TBI research. Nevertheless, the advantages of such an integration are manifold because it can allow the high spatial resolution of MRI/DTI to be combined with the high temporal resolution of EEG and, thereby, to take advantage of all techniques simultaneously (Fig. 5).

The primary sources of EEG potentials are typically currents within the apical dendrites of cortical pyramidal cells [14]; for this reason, EEG generators are assumed to be dipolar currents whose orientations are perpendicular to the cortical surface [15]. In the first step of EEG modeling, finite element method (FEM) models are created by discretizing the head volume of each subject into linear hexahedral isoparametric elements using information provided by the MRI-derived segmentation. A grid-based

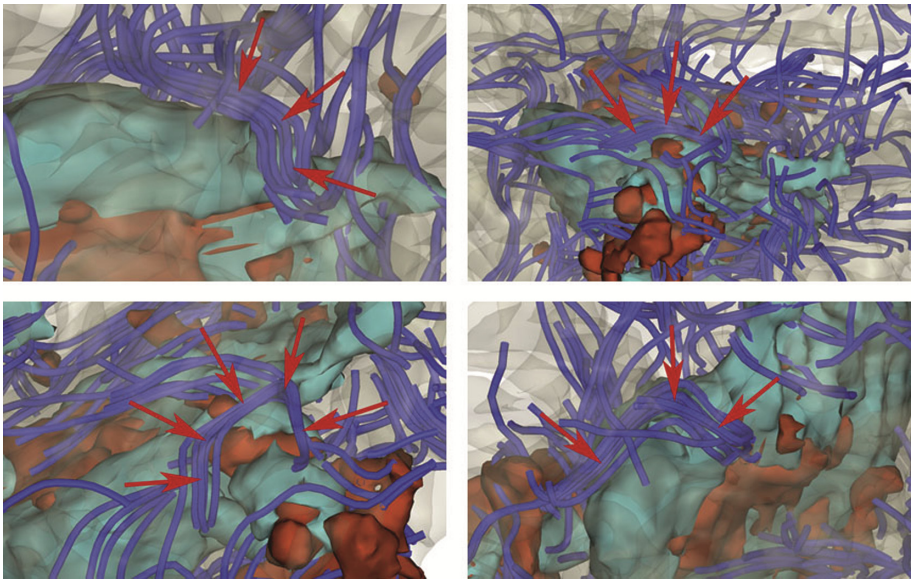

Fig. 3. Detailed views of WM tract deformation (red arrows) due to primary TBI (edema: cyan; hemorrhage: red). Because of the mechanical forces exerted by injuries, WM fibers are subjected to stretching and shearing which lead to diffuse axonal injury (DAI) (Color figure onlilne).

mesh with a mean edge length of ~2 mm, with ~450,000 linear elements and ~400,000 nodes is then generated. After co-registration of the head and sensor locations, the presence of scalp electrodes arranged in the standard 10–10 montage is taken into account and as many as 25 tissue types with distinct conductivity values σ are included.

A TBI-tailored version of the METUFEM software package [16, 17] is used to compute the forward matrix **A** of dimensions $m \times n$, where m and n are the number of sensors and sources, respectively. In each volume element within the head, the electric potential Φ is computed using linear interpolation functions [16]. For a given sensor i and cortical source j, the matrix element a_{ij} of **A** specifies Φ as recorded by sensor i due to a dipolar source of unit strength which is active at the location of source j. Row $\mathbf{a}_i$ of **A** is the so-called 'lead field' (LF) of sensor i, which indicates how each current dipole contributes to the signal recorded by sensor i. Leting $\boldsymbol{J}_p$ denote the primary electric current density of sources in the brain, the solution to the forward problem of electrical source imaging is provided by solving for Φ subject to the boundary conditions

$$\nabla \cdot (\sigma \nabla \boldsymbol{\Phi}) = \nabla \cdot J_p \text{ in } V \tag{1}$$

$$\sigma \, \partial_{\boldsymbol{n}} \boldsymbol{\Phi} = 0 \text{ on } S \tag{2}$$

where V and S are the head volume and surface, respectively, $\boldsymbol{n}$ is the unit normal vector on the surface S, and σ denotes the local tissue conductivity. A point source model [18] is used to assign the desired locations of dipoles within the head. An equivalent discretized model is then constructed for each finite element using Galerkin's weighted

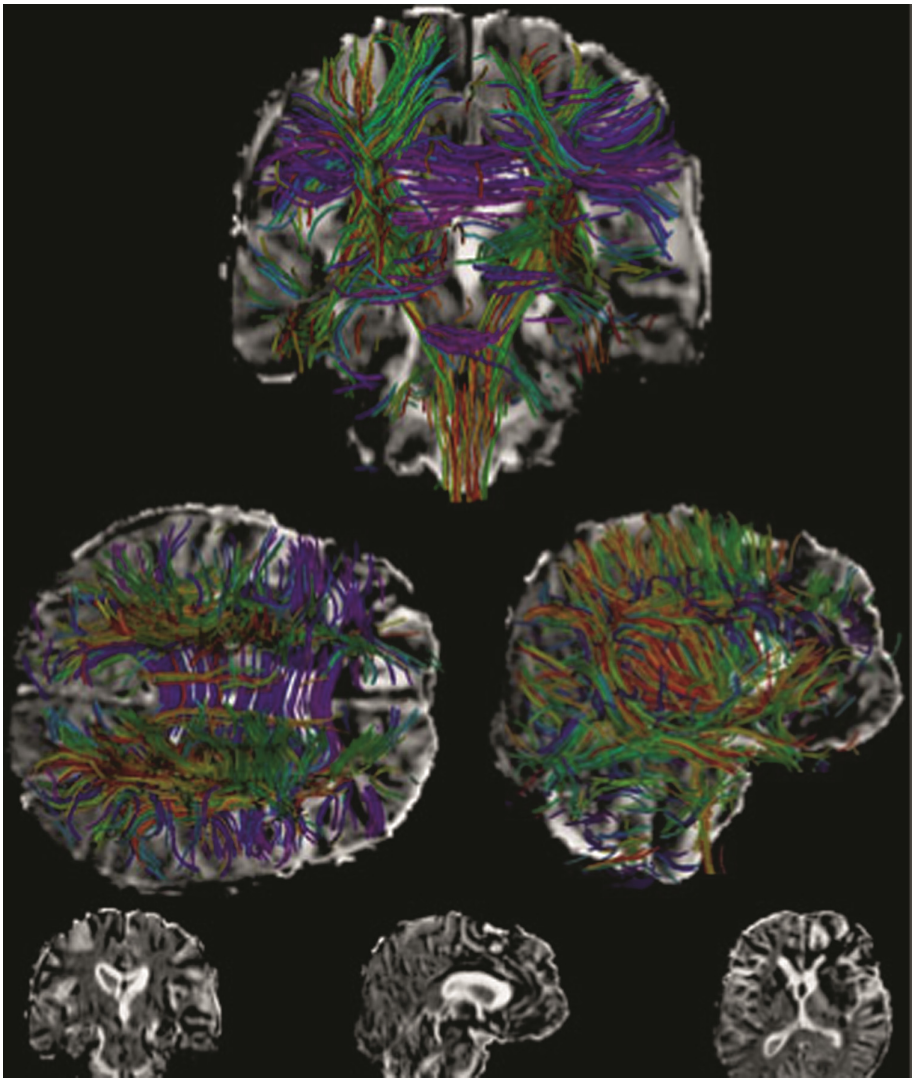

Fig. 4. Sample longitudinal analysis illustrating TBI-related axonal demyelination in a typical patient. Shown are demyelination maps with important WM tracts superimposed. The maps themselves are shown in the bottom row, illustrating substantial demyelination (brighter areas) throughout the brain, especially in peri-ventricular and fronto-temporal areas (Color figure onlilne).

residuals method, and each element contribution is assembled to construct a system of equations whose numerical solution yields the values of Φ [16].

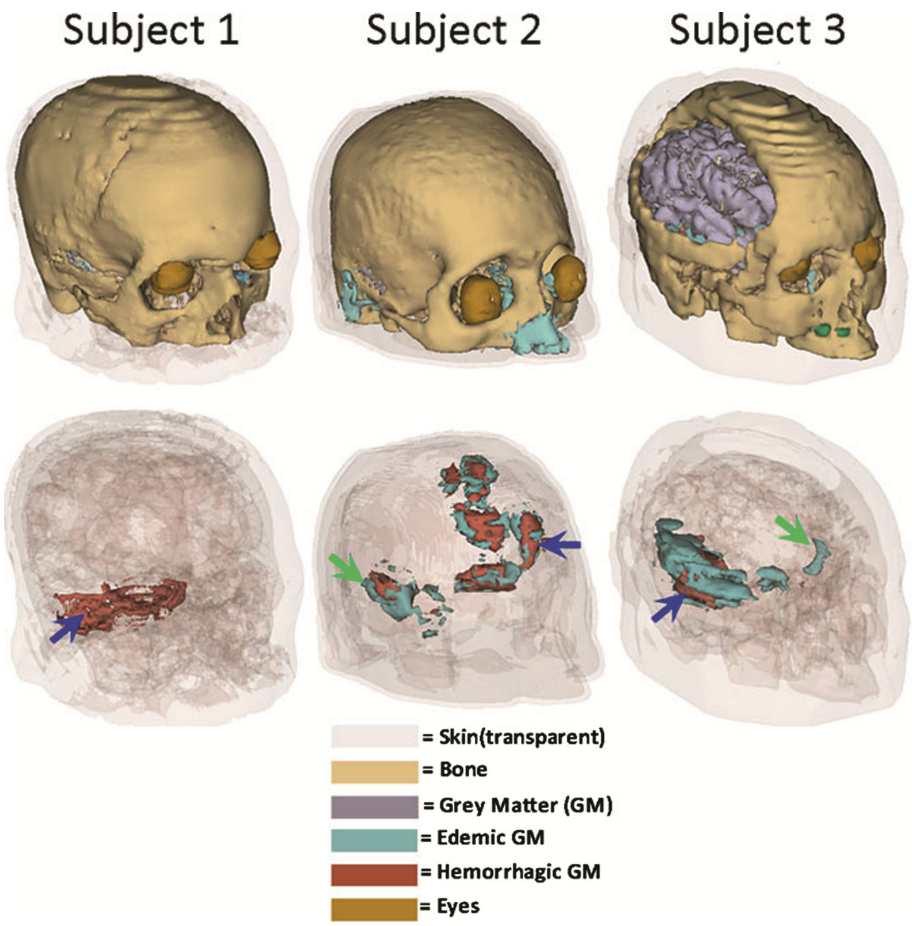

Fig. 5. 3D models of the head for a sample TBI patient. In addition to the full model which includes all tissue types (first row), lesions are shown as well (second row). Hemorrhagic lesions are indicated by blue arrows, while edematous regions are indicated by green arrows. Note the large craniotomy over the right hemisphere of Subject 3, which can be more easily modelled within the FEM formalism as opposed to the boundary element method (BEM) formalism, which requires closed surfaces when approximating the shape of the head (Color figure onlilne).

2.6 EEG Inverse Modeling

The framework for source localization employed here involves a minimum-norm inverse linear operator previously described and widely used [19]. Briefly, one can start from the matrix linear equation

$$\mathbf{x} = \mathbf{A}\mathbf{s} + \mathbf{n}, \tag{3}$$

where **x** is the EEG measurements vector, **A** is the EEG forward matrix, **s** is a vector containing the direction and orientation of each source, and **n** specifies the sensor noise.

To identify **s** from **x** using a linear approach, an inverse operator **W** can be calculated such that the mean difference $\left\langle ||\mathrm{Wx} - \mathrm{s}||^2 \right\rangle$ between the estimated and true inverse solutions is minimal. If **n** and **s** are normally distributed with zero mean, **W** is of the form

$$\mathbf{W} = \mathbf{R}\mathbf{A}^{\mathrm{T}} \left(\mathbf{A}\mathbf{R}\mathbf{A}^{\mathrm{T}} + \mathbf{C} \right)^{-1} \tag{4}$$

where **C** and **R** denote the sensor noise and source covariance matrices, respectively [19]. Normally-distributed white noise can often be assumed for both sources and sensors, such that **R** and **C** are within a constant multiplying factor of the identity matrix.

In EEG inverse localization, the primary interest is in identifying cortical activity whose magnitude is much larger than that of the noise. Because of this, each row of the inverse matrix should be normalized based on the noise sensitivity of **W** at each location [19]. This allows activity at locations with relatively low noise sensitivity to be assigned a greater weight than at locations with higher noise sensitivity. Noise sensitivity estimation can be implemented by projecting the noise covariance estimate onto **W**, such that the noise sensitivity-adjusted inverse operator is pre-multiplied by a diagonal noise sensitivity matrix **T** whose matrix elements t_{ii} are specified by

$$t_{ii} = \left[\mathrm{diag} \left(\sqrt{\mathbf{W}\mathbf{C}\mathbf{W}^{T}} \right) \right]^{-1} \tag{5}$$

and the noise sensitivity-normalized inverse becomes

$$\tilde{\mathbf{W}} = \mathbf{T}\mathbf{W}. \tag{6}$$

Applying the noise-normalized inverse operator to the acquired EEG signals produces a matrix of inversely-localized signals whose rows correspond to cortical locations, whose columns correspond to time points in the EEG recording, and whose units are nAm (electric current dipole strengths). Upon noise normalization, the values of the signals localized on the cortex follow a T distribution with a very large number of degrees of freedom (d. f.) which approaches a normal distribution in the limit d. f. $\rightarrow \infty$. For any given cortical location, the value of the t statistic associated with that location indicates the likelihood that the neuronal source positioned there is electrically active. Cortical maps of t statistics are generated using purpose-built software in order to visualize and identify the cortical areas whose activation is most likely to have produced the EEG signals recorded during each epileptiform discharge.

2.7 Epileptiform Signal Analysis

Epileptic seizures are detected by an NICU nurse or by a neurointensivist within the first week post-injury either online, during EEG screening, or via the total power trend seizure detection approach [3]. To identify interictal epileptiform events, cEEG recordings are examined by a neurophysiologist using custom software. For the purpose of most studies, epileptiform discharges are defined as high-frequency (>80 Hz), high-amplitude (>100 mV) bursts or runs of interictal activity which are not consistent with EEG artifacts due to the following causes: (1) electromyographic activity (20–80 Hz), (2) glossokynetic movement, (3) ocular movement, (4) electrocardiographic activity,

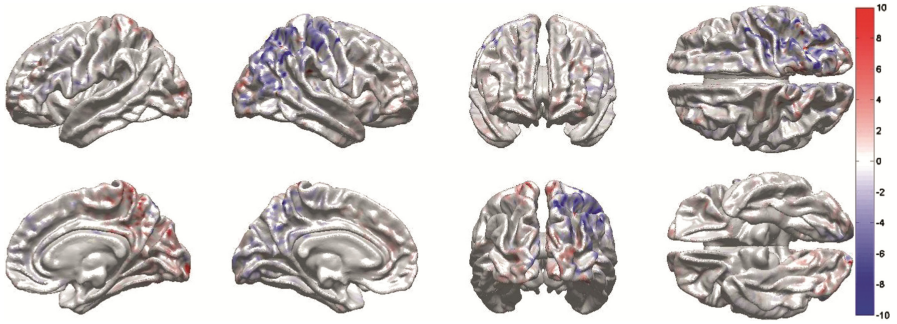

Fig. 6. Example of inversely-localized epileptiform activity in a sample TBI patient. Shown are values of the *t* statistic, as overlayed on the cortical surface. Each *t* statistic indicates the likelihood that the cortex is electrically active at that location. A negative value indicates that the electric current is oriented into the cortex, while a positive value indicates the converse. In this particular case, the presence of a cortical locus of epileptiform electrical activity is found over right parietal cortex.

(5) blood vessel pulsation, (6) respiration, (7) scalp-localized perspiration, (8) electrode disconnection, (9) alternating currents (ACs), and (10) environment-related movement.

Upon identification, all EEG recording segments related to interictal epileptiform events are isolated for subsequent analysis and detrended. Short (~3 s) portions of EEG recordings which either precede or follow each interictal epileptiform event are also saved separately and treated as baseline activity which is used to compute the noise covariance matrix for inverse localization, as described in previous sections. Following the calculation of the noise-normalized inverse operator $\tilde{\mathbf{W}}$, all EEG-recorded neural activity is localized and the cortical location(s) which are most likely to have generated each epileptiform discharge (i.e. their foci) is/are identified by thresholding the cortical map of *t* statistics which had been generated as previously described.

After identifying epileptiform focus locations, the distance(s) between each of these and the location(s) of primary TBI is/are computed. In the first step, a 3D model of each hemorrhagic or edematous lesion is generated based on the MRI-derived segmentation. In the second step, the shortest Euclidian distance D between each focus and the 3D boundary of each lesion is calculated. In the third step, the location of each epileptiform activity focus is labeled as either intra-, peri- or non-lesional based on the distance between it and the lesion(s) (Fig. 6).

2.8 Accommodation of Semantic Conflicts

Implementation of this project has required substantial accommodation of semantic conflicts between data types to support the process of dynamic reconciliation. To provide interoperability between MRI, CT, DTI and EEG data organization systems, semantic reconciliation was provided by integrating data specifications related to the spatial dimension of the structural data (MRI, CT, DTI) with the temporal dimension provided by the neurophysiological data (EEG). Structural and representational differences were found to occur particularly at the interface between approaches to information organization and

mismatched domains. The process of data integration has involved both static schema integration (mapping heterogeneous schemas to a global representation, accounting for context dependencies as precedence relationships during the reconciliation process), as well as dynamic integration (dynamically building appropriate precedence relationships based on already-acquired semantic knowledge).

3 Discussion

From the standpoint of structural neuroimaging data integration, using multimodal data sets which were acquired using different sequences can pose difficulties in several ways. Firstly, due to logistic or technical considerations, imaging volumes cannot always be acquired at the same resolution (i.e. voxel size), which implies that voxel-based multimodal analysis may require 3D interpolation. Secondly, volumes acquired using different modalities may occasionally cover different—though mostly overlapping—FOVs within the brain. From the standpoint of 3D co-registration, this can pose a challenge because the spatial domains containing data to be registered do not feature an identical extent of head coverage. This problem is often compounded when longitudinal scans of the same patient are acquired, typically because the position of the patient's head within the MRI scanner differs across data acquisition sessions. Thirdly, because the problem of patient motion in the scanner is greater for TBI patients than in most other patient populations, motion-related artifacts can be more difficult to correct and thus highly-robust motion correction algorithms and/or scanning sequences are very useful in TBI neuroimaging. Fourthly, because distinct sequences can feature widely different voxel intensity profiles (e.g. in FLAIR vs. SWI), intensity normalization both across modalities and across time points must be implemented with greater care than in other studies. For example, the presence of lesions can be associated with regions of substantial hyper- or hypo-intensities across imaging modalities, which makes the use of histogram-matching algorithms problematic. In our studies, the challenges described above are typically addressed using sophisticated, TBI-tailored interpolation algorithms available within the LONI Pipeline environment which are described in detail elsewhere [20–22].

Integration of structural MRI data with DTI to study TBI in a longitudinal context is challenging because, in addition to substantial changes in overall shape, the TBI brain can also undergo appreciable deformations throughout the WM. Teasing out such deformations from WM losses can be very difficult because the deformation field which indicates how each point in the brain changes its location cannot always be determined with precision. Ideally, a spatially-resolved deformation field which specifies how each point in the brain has moved from one time point to the next should be available. Nevertheless, because some brain changes are diffeomorphic whereas others are not, the deformation field cannot always be determined with accuracy. Additionally, pathology may appear or disappear between time points, which complicates the task even further. As a result, substantial future efforts are required to formulate TBI-robust registration and segmentation methods.

Though there are numerous advantages to the integration of structural (MRI, CT, DTI) neuroimaging with neurophysiological techniques (EEG in the present case), there are substantial difficulties associated with the fusion of such characteristically different types of data. As in our case, overcoming these barriers can involve the use of sophisticated, anatomically-informed methods for inverse localization of electric potentials. Such methods have been in common use by scientists who investigate the healthy brain, though not as common for the study of acute diseases of the brain, and virtually unheard of—until recently—for the study of TBI. Of crucial importance for the successful integration of EEG with structural neuroimaging is the accuracy of the forward models which are used to calculate the inverse localization operator, primarily because the propagation of electric currents which generate the scalp EEG is highly sensitive upon the electric conductivity profile of the head. Thus, it is important to create realistic geometric models of both healthy-appearing and TBI-affected tissues in order to localize epileptiform activity with spatial accuracy. Currently, no automatic algorithms exist for the segmentation of certain tissue types such as fat, muscle, cartilage, connective tissue, or hard/soft bone, which can make the task of creating accurate EEG forward models both difficult and time-consuming. For this reason, renewed efforts by computer scientists and bioengineers are needed in order to develop new or improved methods for the segmentation of various anatomic structures in addition to those located inside the brain.

4 Conclusion

Although potentially difficult, the integration of structural neuroimaging data with neurophysiologic recordings is very useful for studying a variety of disorders and pathologies, including TBI. The use of multimodal neuroimaging of brain injury is very useful—and indeed, essential—to identify, classify and quantify injury types and to generate realistic models of the TBI head which can be used for EEG modeling and inverse localization. Though epileptiform electrical activity is common in the acute stage of TBI, little research has been devoted to understanding the underlying mechanisms of interictal discharges, which may have an important role in the development of post-traumatic epilepsy. The reason for this lack of information is partly due to the difficulty of integrating EEG recordings with other types of neuroimaging which have comparatively higher spatial resolution, such as MRI, CT, DTI and PET. The techniques we have outlined for such integration have provided the ability to obtain useful insights into TBI-related neuropathophysiology, although substantial additional research is needed to develop automatic methods for TBI segmentation as well as for the automatic classification of tissues which play important roles in the accurate inverse localization of electric potentials.

Acknowledgments. This work was supported by the National Institutes of Health, grants 2U54EB005149-06 “National Alliance for Medical Image Computing: Traumatic Brain Injury – Driving Biological Project” to J. D. V. H., and R41NS081792-01 “Multimodality Image Based Assessment System for Traumatic Brain Injury”, sub-award to J. D. V. H, and by the National Institute of Neurological Disorders and Stroke, grant P01NS058489 to P.M.V. We wish to thank

the dedicated staff of the Institute for Neuroimaging and Informatics at the University of Southern California. The authors declare no actual or perceived competing conflict of interest.

References

1. Dale, A.M., Sereno, M.I.: Improved localizadon of cortical activity by combining EEG and MEG with MRI cortical surface reconstruction: a linear approach. J. Cogn. Neurosci. **5**, 162–176 (1993)
2. Brophy, G.M., Bell, R., Claassen, J., Alldredge, B., Bleck, T.P., Glauser, T., Laroche, S.M., Riviello Jr., J.J., Shutter, L., Sperling, M.R., Treiman, D.M., Vespa, P.M.: Neurocritical care society status epilepticus guideline writing, C.: guidelines for the evaluation and management of status epilepticus. Neurocrit. Care **17**, 3–23 (2012)
3. Vespa, P.M., Nuwer, M.R., Nenov, V., Ronne-Engstrom, E., Hovda, D.A., Bergsneider, M., Kelly, D.F., Martin, N.A., Becker, D.P.: Increased incidence and impact of nonconvulsive and convulsive seizures after traumatic brain injury as detected by continuous electroencephalographic monitoring. J. Neurosurg. **91**, 750–760 (1999)
4. Irimia, A., Chambers, M.C., Alger, J.R., Filippou, M., Prastawa, M.W., Wang, B., Hovda, D.A., Gerig, G., Toga, A.W., Kikinis, R., Vespa, P.M., Van Horn, J.D.: Comparison of acute and chronic traumatic brain injury using semi-automatic multimodal segmentation of MR volumes. J. Neurotrauma **28**, 2287–2306 (2011)
5. Dale, A.M., Fischl, B., Sereno, M.I.: Cortical surface-based analysis – I. segmentation and surface reconstruction. NeuroImage **9**, 179–194 (1999)
6. Fischl, B., Sereno, M.I., Dale, A.M.: Cortical surface-based analysis - II: inflation, flattening, and a surface-based coordinate system. Neuroimage **9**, 195–207 (1999)
7. Fischl, B., Salat, D.H., Busa, E., Albert, M., Dieterich, M., Haselgrove, C., van der Kouwe, A., Killiany, R., Kennedy, D., Klaveness, S., Montillo, A., Makris, N., Rosen, B., Dale, A.M.: Whole brain segmentation: automated labeling of neuroanatomical structures in the human brain. Neuron **33**, 341–355 (2002)
8. Destrieux, C., Fischl, B., Dale, A., Halgren, E.: Automatic parcellation of human cortical gyri and sulci using standard anatomical nomenclature. Neuroimage **53**, 1–15 (2010)
9. Fischl, B., Salat, D.H., van der Kouwe, A.J., Makris, N., Segonne, F., Quinn, B.T., Dale, A.M.: Sequence-independent segmentation of magnetic resonance images. NeuroImage **23**(Suppl 1), S69–S84 (2004)
10. Irimia, A., Chambers, M.C., Alger, J.R., Filippou, M., Prastawa, M.W., Wang, B., Hovda, D.A., Gerig, G., Toga, A.W., Kikinis, R., Vespa, P.M., Van Horn, J.D.: Comparison of acute and chronic traumatic brain injury using semi-automatic multimodal segmentation of MR volumes. J. Neurotrauma **28**, 2287–2306 (2011)
11. Irimia, A., Chambers, M.C., Torgerson, C.M., Filippou, M., Hovda, D.A., Alger, J.R., Gerig, G., Toga, A.W., Vespa, P.M., Kikinis, R., Van Horn, J.D.: Patient-tailored connectomics visualization for the assessment of white matter atrophy in traumatic brain injury. Front. Neurol. **3**, 10 (2012)
12. Jenkinson, M., Beckmann, C.F., Behrens, T.E., Woolrich, M.W., Smith, S.M.: Fsl. Neuroimage **62**, 782–790 (2012)
13. Glasser, M.F., Van Essen, D.C.: Mapping human cortical areas in vivo based on myelin content as revealed by T1- and T2-weighted MRI. J. Neurosci. **31**, 11597–11616 (2011)
14. Dale, A., Sereno, M.: Improved localization of cortical activity by combining EEG and MEG with MRI cortical surface reconstruction: a linear approach. J. Cogn. Neurosci. **5**, 162–176 (1993)

15. Irimia, A., Van Horn, J.D., Halgren, E.: Source cancellation profiles of electro encephalography and magnetoencephalography. Neuroimage **59**, 2464–2474 (2012)
16. Acar, Z., Gencer, N.: An advanced BEM implementation for the forward problem of electromagnetic source Imaging. Phys. Med. Biol. **49**, 5011–5028 (2004)
17. Acar, Z., Makeig, S.: Neuroelectromagnetic forward head modeling toolbox. J. Neurosci. Methods **190**, 258–270 (2010)
18. Yan, Y., Nunez, P.L., Hart, R.T.: Finite-element model of the human head: scalp potentials due to dipole sources. Med. Biol. Eng. Comput. **29**, 475–481 (1991)
19. Liu, A.K., Dale, A.M., Belliveau, J.W.: Monte Carlo simulation studies of EEG and MEG localization accuracy. Hum. Brain Mapp. **16**, 47–62 (2002)
20. Wang, B., Prastawa, M., Irimia, A., Chambers, M.C., Vespa, P.M., Van Horn, J.D., Gerig, G.: A patient-specific segmentation framework for longitudinal MR images of traumatic brain injury. In: Proceedings of Spie 8314 (2012)
21. Wang, B., Prastawa, M., Irimia, A., Chambers, M.C., Sadeghi, N., Vespa, P.M., van Horn, J.D., Gerig, G.: Analyzing imaging biomarkers for traumatic brain injury using 4d modeling of longitudinal MRI. In: I S Biomed Imaging, pp. 1392–1395 (2013)
22. Wang, B., Prastawa, M., Awate, S.P., Irimia, A., Chambers, M.C., Vespa, P.M., van Horn, J.D., Gerig, G.: Segmentation of serial MRI of TBI patients using personalized atlas construction and topological change estimation. In: 2012 9th IEEE International Symposium on Biomedical Imaging (Isbi), pp. 1152–1155 (2012)